JOURNAL OF CATALYSIS **161,** 471–479 (1996)
ARTICLE NO. 0206

Electrochemical Promotion by Na of the Platinum-Catalyzed Reaction between CO and NO

Alejandra Palermo,[1] Richard M. Lambert,[2] Ian R. Harkness,[3] Ioannis V. Yentekakis,* Olga Mar'ina,*,[4] and Constantinos G. Vayenas*

*Department of Chemistry, University of Cambridge, Cambridge CB2 1EW, England; and *Department of Chemical Engineering, University of Patras, Patras, GR-26500, Greece*

Received October 9, 1995; revised February 1, 1996; accepted February 5, 1996

The Pt-catalyzed reduction of NO by CO exhibits strong electrochemical promotion (EP) by backspillover Na supplied from β'' alumina under appropriate conditions of temperature, gas composition, and catalyst potential. At high CO partial pressures (P_{CO}) the EP effect is attenuated by CO island formation and limited availability of chemisorbed NO. At low P_{CO}, the CO + O reaction is limited by the low coverage of CO and the EP effect is again relatively small. In the intermediate P_{CO} regime, Na pumping strongly accelerates the reaction: rate gains of up to 1300% for N_2 production, relative to the unpromoted rate are observed. This can be understood in terms of Na-induced dissociation of chemisorbed molecular NO, which is thought to be the reaction initiating step. The overall kinetic behavior and the dependence of N_2/N_2O selectivity on catalyst potential are in good accord with this hypothesis. Thus the EP system also provides direct information about the nature of the reaction mechanism under conditions of elevated pressure.

INTRODUCTION

Non-Faradaic electrochemical modification of catalytic activity (NEMCA) or electrochemical promotion (EP) has been described for many catalytic reactions on Pt, Pd, Rh, Au, Ag, and IrO_2 surfaces and the subject has been extensively reviewed (see Ref. (1) and references therein). The phenomenon occurs when catalytic reactions take place on a variety of metal films in contact with a solid electrolyte, where the latter acts as a source of electrochemically controlled promoter species that directly modify the behavior of the catalyst film (the working electrode). Recently, Vayenas and co-workers demonstrated the effect with a liquid electrolyte where the behavior was entirely analogous to that exhibited by solid electrolyte systems (2). These EP systems are characterized by a very large value of the ratio between the change in turnover rate and the rate of charge transport through the electrolyte (up to 10^5). Reported gains in reaction rate with respect to the unpromoted rate lie in the range 2–100 (3).

Vayenas *et al.* have advanced a theoretical model which provides a very satisfactory quantitative account of the EP effect (1). It is proposed that backspillover ions pumped from the solid electrolyte modify the catalyst surface work function, as confirmed experimentally (1), with concomitant changes in adsorption enthalpies and reaction activation energies. This in turn can lead to major changes in catalytic activity and selectivity. Useful information about the reacting system can be obtained in either of two modes: measurements of the steady-state reaction rate under *potentiostatic* conditions provide information about kinetics and mechanism: transient (*galvanostatic*) measurements show how the time dependence of promoter-induced changes in catalyst potential correlate with changes in catalytic rate. In the present case, galvanostatic data are also used to calibrate the Na coverage scale.

Here we describe an EP study of the CO + NO reaction over Pt/β'' alumina. The Pt-catalyzed oxidation of CO by dioxygen is one of the most extensively studied systems and it is well established that the reaction proceeds by a Langmuir–Hinshelwood mechanism (4); an EP study of this reaction over Pt/β'' alumina has already been published (5). The CO + NO reaction is of importance with regard to pollution abatement in that it involves simultaneous removal of two toxic species. Rh, though costly, is the preferred catalyst for this reaction because of its superior ability to dissociatively chemisorb NO, a process for which Pt is normally a relatively poor catalyst. Although most earlier work indicates that NO dissociation is the rate limiting step in the Pt-catalyzed reaction (6–8), the authors of a more recent kinetic study concluded that the reaction occurs by a

[1] Current address: Institute of Materials Science and Technology (INTEMA), UNMDP-CONICET, J.B. Justo 4302, (7600) Mar del Plata, Argentina.

[2] To whom correspondence should be addressed. Fax: 44 1223 336362. E-mail: rml1@cam.ac.uk.

[3] Current address: Chemistry Department, Edinburgh University, Edinburgh EH9 3JJ.

[4] Current address: Boreskov Institute of Catalysis, Novosibirsk 630090, Russia.

0021-9517/96 $18.00

non-dissociative mechanism involving direct interaction between CO and NO molecules (9). Even though the CO + NO reaction over Pt has been extensively studied over a range of conditions and with a variety of catalysts ranging from single crystals (6, 7, 10–12) to practical dispersed materials (8, 13–16) there have been no previous studies of the effects of alkali promotion, a phenomenon whose importance is widely recognized in non-EP systems (17). Electrochemical promotion of a Pt film using an active (ion conducting) β'' alumina support provides a uniquely effective way of examining the effects of Na promotion in a controllable and reversible manner. Large changes in catalyst activity and selectivity can be induced and our results strongly favor the dissociative mechanism for NO reduction: the variation of activity and selectivity with catalyst potential both point to NO dissociation as the key reaction initiating step.

METHODS

The catalyst (working electrode) consisted of a porous but continuous thin Pt film deposited on the a 20-mm-diameter disc of β''-Al_2O_3 as described in detail elsewhere (18), i.e., by using a thin coating of Engelhard Pt A1121 paste followed by calcination in air first at 723 K for 1 h and then at 1023 K for 30 min. O_2, CO surface titration (19) at 620 K gave a value of 1.15×10^{-6} mol of Pt for the active metal area of the resulting film. Au reference and counterelectrodes were attached to the other face of the β''-Al_2O_3 wafer using an Au paste prepared by mixing Aldrich Au powder (99.9%+) in a slurry of polyvinyl acetate binder in ethyl acetate, followed by calcination at 1023 K. The β''-Al_2O_3 disc was suspended in a quartz well-mixed reactor with all three electrodes exposed to the reactant gas mixture (Fig. 1). The quartz reactor volume was 25 cm^3 and the performance of this type of single pellet CST reactor has been described and discussed elsewhere (20). On-line gas chromatography was used for analysis of reactants and products (N_2O, NO, CO, and CO_2), as previously described (5). CO_2 was also continuously monitored with an IR analyzer (ANARAD AR-500 CO_2 Analyzer). The carbon mass balance was found to close within 2%. Quoted N_2 rates (r_{N_2}, were computed from the measured CO_2 and N_2O rates ($r_{N_2} = (r_{CO_2} - r_{N_2O})/2$) according to the following stoichiometric equations:

$$NO + CO \rightarrow CO_2 + \tfrac{1}{2}N_2 \quad [1]$$

$$2NO + CO \rightarrow CO_2 + N_2O. \quad [2]$$

Catalytic rate measurements under potentiostatic or galvanostatic conditions were carried out using a galvanostat potentiostat (Amel type 553), the galvanostatic transient behavior of V_{WR} being used to calibrate the Na coverage scale. Most experiments were carried out in the potentiostatic mode by following the effect of the potential difference between the catalyst and the reference electrode (V_{WR}) on the reaction rate. The reactant gas mixture was delivered at total flowrates of $1–2 \times 10^{-4}$ mol s^{-1}, with partial pressures P_{NO} and P_{CO} varied between 0 and 1.5 and 0 and 1.5 kPa, respectively, and with P_{He}, giving a total pressure of 1 atm in every case. Conversion of the reactants was typically ~15%. CO was passed through a heated quartz trap at 570 K to eliminate possible contamination by Fe carbonyl. Control experiments confirmed that the Au reference and counterelectrodes were catalytically inert under all conditions. It is worth noting that with the single pellet reactor (1, 5, 20, 21) the "reference" electrode is, strictly speaking, a pseudoreference electrode—since its potential is not pinned to a thermodynamically well-defined value. However, this is not a serious drawback since it is knowledge of *changes* in potential (and thus work function (1)) that is required for a description of the observed promotional phenomena. The potential of the Au pseudoreference electrode does not change appreciably with changing gaseous composition, as can be inferred by comparing EP results for ethylene oxidation over Pt/β'' alumina obtained with the single pellet design (21) and with the fuel cell type design, i.e., with the reference electrode exposed to ambient air (22). In the two cases, a sharp decrease in rate occurred over essentially the same (±0.2 V) range of V_{WR}.

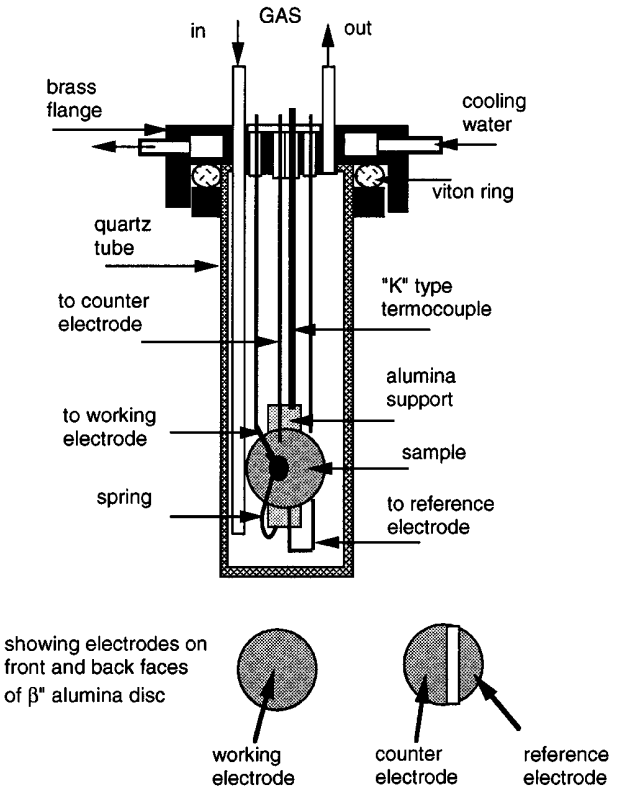

FIG. 1. Single pellet catalytic reactor and electrodes configuration.

RESULTS

Behaviour under a Galvanostatic Transient

In order to obtain an estimate of the Na coverage corresponding to any given value of V_{WR}, galvanostatic transients were obtained and analyzed as described previously by Vayenas *et al.* (22). First, the surface was electrochemically cleaned of Na by application of a positive potential (V_{WR}) in the order of 400 mV until the current between the catalyst and counterelectrode vanished. Then, the galvanostat was used to impose a constant current $i = -50\ \mu$A at $t = 0$; this pumped Na to the catalyst surface at a rate $I/F = 5.18 \times 10^{-10}$ mol Na/s. The corresponding Na coverage on the Pt surface (θ_{Na}) can be computed from Faraday's Law; i.e.,

$$\frac{d\theta_{Na}}{dt} = -\frac{I}{FN}, \qquad [3]$$

where $N(= 1.15 \times 10^{-6}$ mol Pt) is the number of available Pt sites independently measured by surface titration.

Galvanostatic measurements also provide a rapid method for assessing the response of the reaction rate to Na pumping over a range of conditions. Figure 2a shows the behavior of the CO_2 rate and corresponding changes in catalyst potential under a galvanostatic transient for a 1:1 CO:NO mixture. Under these conditions, Na pumping to the catalyst leads to a large step change in reaction rate (r) which is complete at a sodium coverage (θ_{Na}) of ~0.03 at which point the catalyst potential (i.e., the work function (1)) has decreased by ~0.6 eV. This rapid initial response of the rate to Na pumping may be conveniently specified in terms of the promotion index defined (5) as $P_{Na} = (\Delta r/r_0)/\Delta\theta_{Na}$. In this initial regime the promotion index is near 200 (Fig. 2a) which is the largest value observed so far, though of the same order as that observed in the Na-induced electrochemical promotion of the $CO + O_2$ reaction (5). Thereafter the rate and potential remain essentially constant over a substantial range of Na coverage. Figure 2b shows a family of galvanostatic transients obtained for a range of CO partial pressures at fixed NO inlet

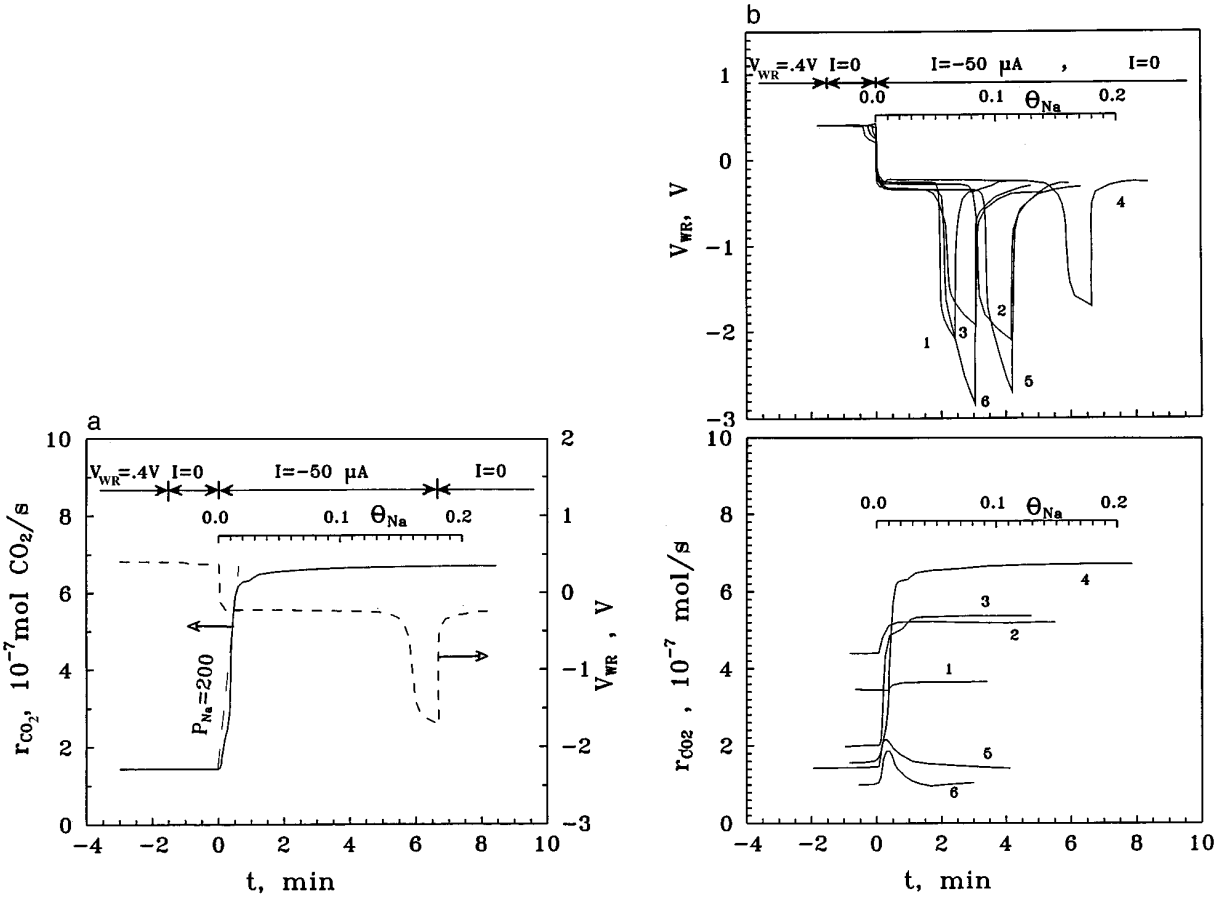

FIG. 2. (a) Typical galvanostatic transient showing the effect of a step change of the applied current on the CO_2 formation rate (solid line) and on the catalyst potential V_{WR} (dotted line) as a function of time. Conditions: $T = 621$ K, $P^0_{NO} = P^0_{CO} = 0.75$ kPa. (b) Typical galvanostatic transient at different gas composition in the reactor cell, showing the effect of the applied current ($-50\ \mu$A) on the catalyst potential (top) and CO_2 formation rate (bottom) as a function of time. Conditions: $P^0_{NO} = 0.75$ kPa, $T = 621$ K; (1) $P^0_{CO} = 0.37$ kPa, (2) $P^0_{CO} = 0.55$ kPa, (3) $P^0_{CO} = 0.62$ kPa, (4) $P^0_{CO} = 0.75$ kPa, (5) $P^0_{CO} = 1.0$ kPa, (6) $P^0_{CO} = 1.2$ kPa.

pressure $P^0_{NO} = 0.75$ kPa. It is apparent that both the intensity and the persistence of the EP effect as a function of increasing Na coverage are strongly dependent on the composition of the reactant gas mixture. Close to stoichiometry one observes pronounced "S"-type rate behavior with respect to Na coverage; CO-rich mixtures give rise to "volcano" rate curves and NO-rich mixtures produce S-type behavior and only a weak EP effect. As will be shown below, this trend in behavior is mirrored exactly by the potentiostatic steady-state data.

Effect of V_{WR} on Reaction Rate under Potentiostatic Conditions

Steady-state measurements of NO decomposition in the absence of CO under potentiostatic conditions gave the expected result, namely rapid self-poisoning of the system by chemisorbed oxygen: addition of CO resulted immediately in a finite reaction rate which varied reversibly and reproducibly with changes in catalyst potential (V_{WR}) and reactant partial pressures. Figure 3 shows steady-state (potentiostatic) rate data for CO_2, N_2, and N_2O production as a function of the V_{WR} at 621 K for a constant inlet pressures (P^0_{NO}, P^0_{CO}) of NO and CO of 0.75 kPa. Also shown in Fig. 3 is the V_{WR} dependence of N_2 selectivity where the latter quantity is defined as

$$S_{N_2} = \frac{r_{N_2}}{r_{N_2} + r_{N_2O}}. \quad [4]$$

Note that there is a sharp increase in activity as V_{WR} is reduced below ~0.2 V (Na pumping *toward* the Pt catalyst) with a concomitant threefold enhancement in the selectivity to N_2. The N_2O rate actually goes through a maximum at $V_{WR} = -0.2$ V. Control experiments were carried out in which the total flow rate was varied by a factor of 2 in order to check that the observed step change in activity is due to a true increase in catalyst activity and is not influenced by mass transfer limitations or by multiple steady states in the reactor.

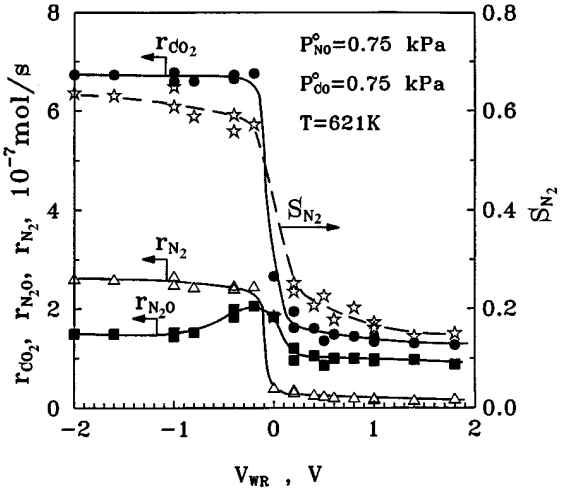

FIG. 3. Effect of catalyst potential (V_{WR}) on the CO_2, N_2, N_2O formation rates and the selectivity of NO reduction to nitrogen. Conditions: $T = 621$ K, $P^0_{NO} = P^0_{CO} = 0.75$ kPa.

Figures 4a–4d show (621 K) potentiostatic rate data for the rates of formation of CO_2, N_2, N_2O and for the N_2 selectivity, S_{N_2}, as a function of inlet pressure of CO, for a fixed NO inlet pressure of 0.75 kPa. Rates are also expressed as turnover frequency (TOF), i.e., moles of product per Pt surface atom per second. In every case the system was perfectly reversible and exhibited no hysteresis when switching between negative (high rates) to positive (low rates) potentials. It is apparent that the EP effect is pronounced at intermediate CO partial pressures and attenuated at high and low CO partial pressures. Note also that this steady-state dependence of the system response on the gas composition mirrors exactly the transient behavior observed under galvanostatic conditions (Fig. 2b). The corresponding selectivity data are shown in Fig. 5d which demonstrates that high levels of Na always increase the selectivity toward N_2. The maximum obtained ρ values are 13 and 1.5 for N_2 and N_2O, respectively, at a gas composition of $P^0_{NO} = P^0_{CO} = 0.75$ kPa. For $P^0_{CO} = 0.75$ kPa, Na pumping to the catalyst leads to an increase in S_{N_2} by up to a factor of three. Note that for low P_{CO} values, increasing Na coverage suppresses the rate of N_2O formation (Fig. 4c).

Effect of P_{CO} and P_{NO} on Promoted and Unpromoted Steady-State Rates

The dependence of the CO_2, N_2, and N_2O rates on P_{CO} at fixed P_{NO} for three different values of the catalyst potential is illustrated in Figs. 5a–5c. $V_{WR} = +1000$ mV corresponds to the clean Pt surface (unpromoted rate) and $V_{WR} = -200$ mV corresponds to a sodium promoted surface. Figure 5d shows the corresponding S_{N_2} data: it is apparent that the highest selectivities to nitrogen production always occur in the presence of the highest Na loading (most negative potential). From Figs. 5a and 5b it can be seen that the CO_2 and N_2 rates exhibit Langmuir-Hinshelwood behavior and that increased levels of Na result in a systematic increase in the CO partial pressure (P^*_{CO}) necessary for inhibition. That is, Na pumping favors the chemisorption of NO relative to CO. The N_2O rate also exhibits Langmuir–Hinshelwood kinetics, but the effect of increased Na is somewhat different: in particular, high levels of Na tend to suppress the N_2O rate and there is no systematic shift in P^*_{CO}. Figures 6a–6d show corresponding results for the dependence of r_{CO_2}, r_{N_2}, r_{N_2O}, and S_{N_2} on P_{NO} at fixed P_{CO} for three different values of catalyst potential. The higher the Na coverage, the lower the NO pressure at which the activity shows a step increase, and no rate maximum is observed within the accessible P_{NO} range.

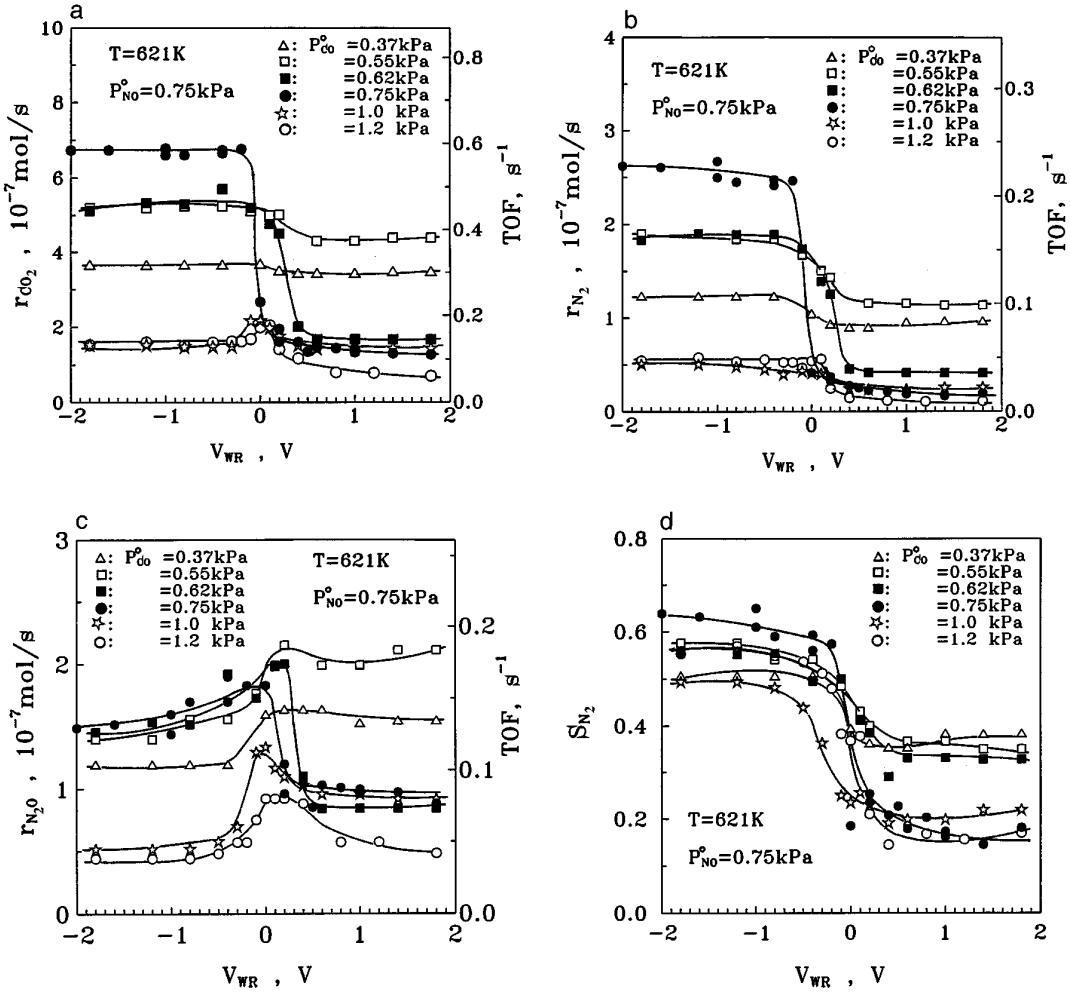

FIG. 4. Effect of catalyst potential (V_{WR}) on the rate of CO_2 (a), N_2 (b), and N_2O (c) formation and on the selectivity of NO reduction to nitrogen (d). Note: Conditions are shown in the figures.

Figure 7a shows Arrhenius plots of the CO_2 rate for stochiometric CO : NO at five different values of catalyst potential over the temperature interval 560–675 K. Three features are apparent: (i) there is a marked change in the apparent activation energy at ~600 K; (ii) the higher the Na loading, the lower the temperature at which this change occurs; (iii) the activation energy associated with the low temperature regime increases monotonically with the Na coverage; the activation energy associated with the high temperature regime is independent of Na coverage. For purposes of comparison, we obtained similar data for the $CO + O_2$ reaction. Figure 7b shows the dependence of the apparent activation energy for CO_2 formation for both reactions ($CO + NO$ and $CO + O_2$) as a function of catalyst potential. It can be seen that these two systems behave similarly in both the high and low activation energy regimes.

DISCUSSION

In the discussion that follows use is made of the term "Na overage." This does not imply that the promoter is thought to be present in the form of chemisorbed metallic sodium as it would be in vacuum; the reactive gas atmosphere is expected to lead to the formation of surface compounds of Na, and single crystal data indicate that stable Na–CO complexes (23) or Na carbonates (24) are formed, depending on the composition of the ambient gas. In the presence of NO, formation of nitroxy surface species is also a plausible possibility. However, our recent work on Pt{111}/NO, O_2, NO_2, CO_2 (25) shows that although alkali nitrite formation is possible under certain conditions, the presence of CO_2(g) leads to formation of the thermodynamically favored carbonate. Adsorbed polar alkali compounds lead to large decreases in work function, of the same order as those produced by

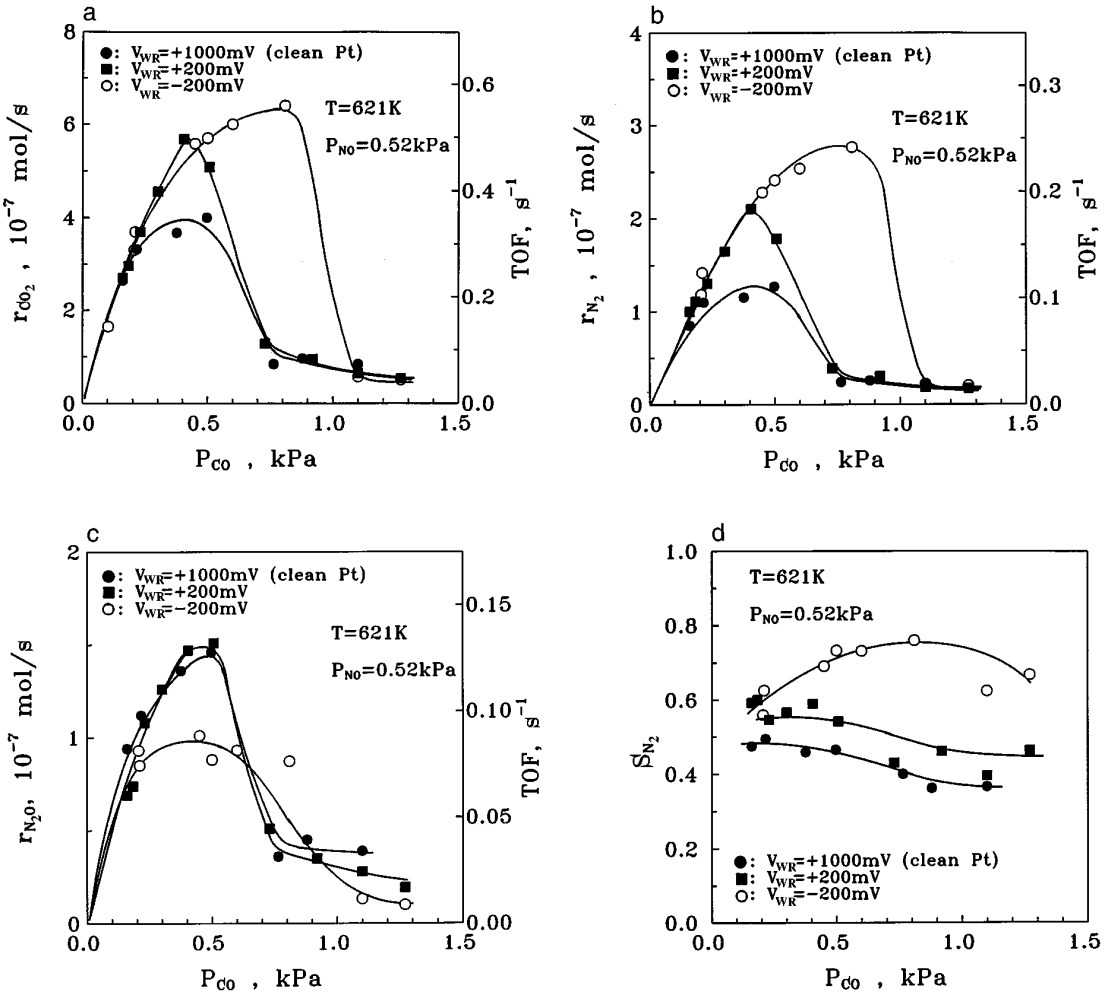

FIG. 5. Effect of partial pressure of CO (P_{CO}) on the rates of CO_2 (a), N_2 (b), and N_2O (c), formation, and on the selectivity of NO reduction to nitrogen (d), at three different fixed catalyst potentials. $T = 621$ K, $P_{NO} = 0.52$ kPa.

the alkali metal itself, so that the general theory of electrochemical promotion (1) is applicable.

The kinetic response of the CO + NO reaction to electrochemical promotion by Na pumping exhibits several differences from the simpler CO + O_2 reaction (5). In the latter case, depending on the conditions, the system exhibits either poisoning alone (S-type behavior) or both promotion and poisoning (volcano-type behavior) as Na is progressively supplied to the catalyst. Promotion is associated with strengthening of the Pt–O bond in the CO-inhibited regime, whereas poisoning is ascribed to site blocking by Na–CO complexes (5).

In the present case r_{CO_2} exhibits both "inverse" S-type and volcano behavior (Figs. 3 and 4a) depending on the gas composition. It is apparent from Fig. 4a that the EP effect is small at low P_{CO}. In this regime the reaction rate is first order in CO and oxygen scavenging from the surface by CO, rather than the extent of NO dissociation, is the dominant factor: Na pumping therefore has little effect as was also the case in CO oxidation for low P_{CO} (5). At high P_{CO} the EP effect is again attenuated: at first, Na pumping induces some promotion, higher Na coverages lead to poisoning. The origin of the relatively weak promotion has been discussed above; the poisoning that characterises the high P_{CO} data we ascribe to site blocking by large CO islands and Na–CO surface complexes, as discussed extensively in our earlier work on the Na-promoted CO + O_2 reaction over Pt (5).

The V_{WR} dependence of r_{N_2O} may be rationalized as follows. N_2O is produced by the surface reaction

$$N_{(a)} + NO_{(a)} \rightarrow N_2O. \qquad [5]$$

The proposed role of Na is as follows. It enhances the adsorption of NO versus CO and promotes NO

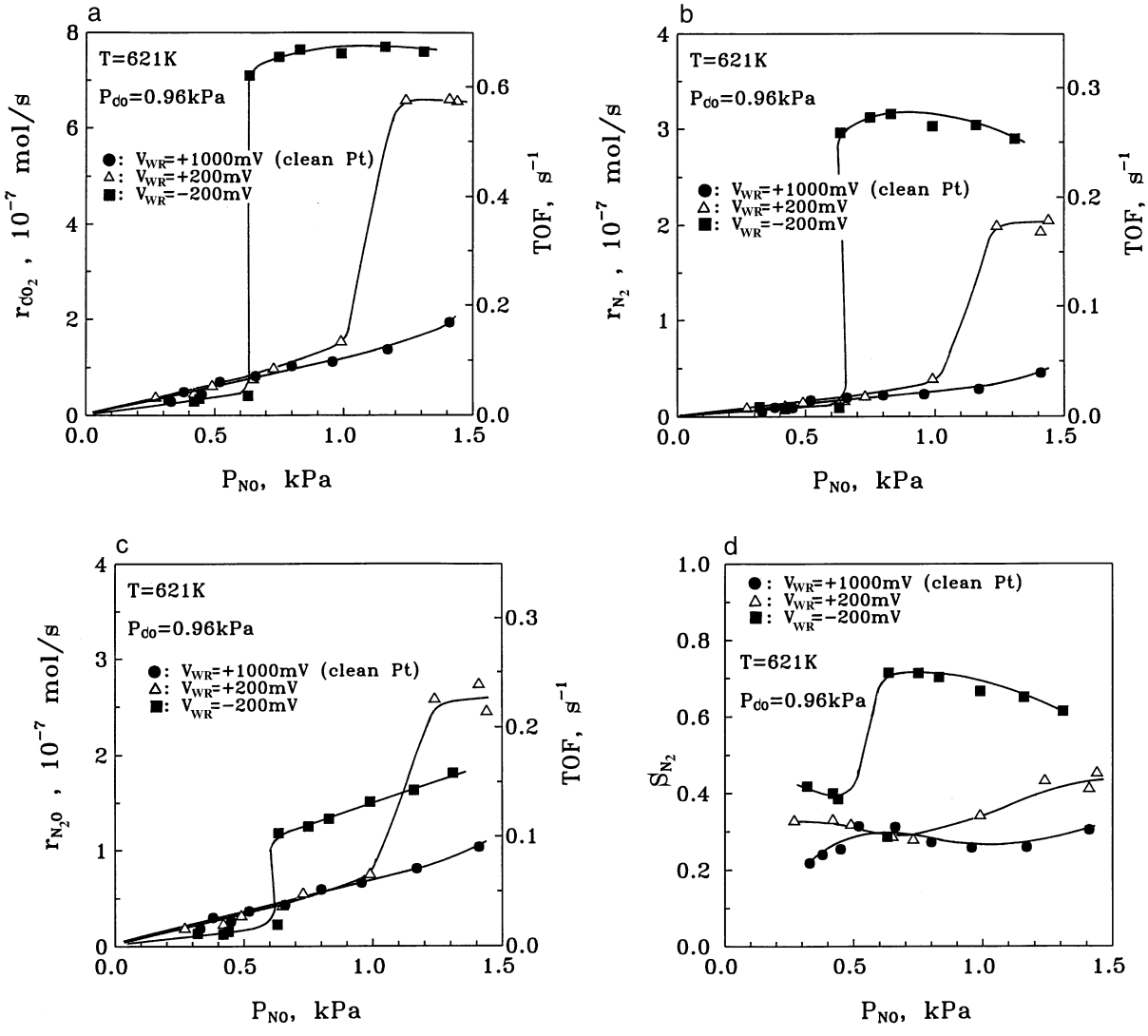

FIG. 6. Effect of partial pressure of NO (P_{NO}) on rates of CO_2 (a), N_2 (b), and N_2O (c) formation, and on the selectivity of NO reduction to N_2 (d), at three different fixed catalyst potentials. $T = 621$ K, $P_{CO} = 0.96$ kPa.

dissociation (24). For high θ_{Na} values (i.e., high Na coverages, $V_{WR} < -0.5$ V Fig. 4c) NO dissociation is extensive and the rate of reaction (5) is diminished for all P_{CO} values due to the limited availability of molecular NO on the surface. This is the dominant effect for low P_{CO} values (Fig. 4c) since in this case the surface is already covered predominantly with NO (versus CO) even for positive potentials. For high P_{CO} values, however, the effect of enhanced NO chemisorption is manifested for intermediate V_{WR} values, due to the low coverage of NO. Consequently, the volcano type behavior (Fig. 4c) of r_{N_2O}, which quantity is proportional to $\theta_{NO} \cdot \theta_N$, is due to the low values of θ_{NO} and θ_N to the left and right of the volcano, respectively.

For intermediate values of P_{CO} (CO : NO ~ 1) where the amounts of NO and CO adsorbed are comparable (as confirmed by the kinetic data in Fig. 5a) the extent of NO dissociation is the key factor in determining the overall rate and so Na supply induces a large EP effect. The r_{N_2} results (Fig. 4b) qualitatively resemble the r_{CO_2} data; r_{N_2O} shows either volcano or inverse S-type behavior as the Na coverage is increased (Fig. 4c). This latter effect is of course responsible for the large step increase in S_{N_2} that occurs at high Na coverages (Fig. 4d); it is also significant from a mechanistic point of view (see below).

The progressive increase in P^*_{CO} with decreasing catalyst potential (increasing Na; Figs. 5a, 5b) is consistent with the view that sodium increases the strength of NO adsorption relative to CO; as noted above, this also implies an increased degree of NO dissociation due to weakening of the N–O bond (26). In line with this, single crystal data demonstrate directly that Na induces NO dissociation on Pt(111) (24, 25). The r_{N_2O} data (Fig. 5c) differ from the r_{CO_2} and r_{N_2} data in

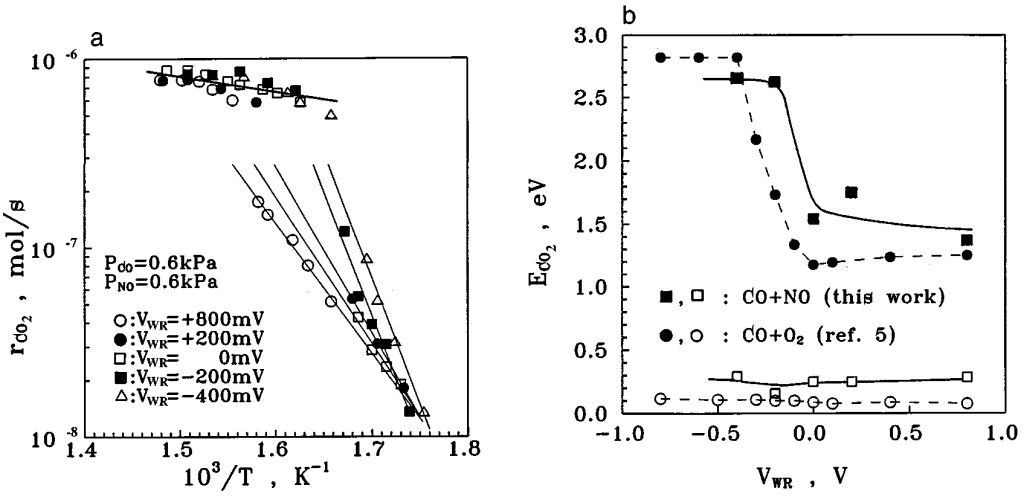

FIG. 7. Arrhenius plots for the CO_2 formation rate at several fixed catalyst potentials (a) and dependence of the apparent activation energy for the formation of CO_2 on the catalyst potential (V_{WR}). $P_{CO} = P_{NO} = 0.6$ kPa. (b) Comparison with previous results referring to the CO oxidation on Pt-β'' alumina (Ref. 5) (see text for discussion).

that the clean Pt surface exhibits higher activity than the Na promoted surface, reflecting the fact that high levels of NO dissociation actually inhibit N_2O formation from N + NO.

This Na-induced increase in binding and dissociation of NO are responsible for the step increase in N_2 and CO_2 activity (Figs. 6a, 6b). The effect is both large ($\rho(\max)_{CO_2} \sim 4.8$; $\rho(\max)_{N_2} \sim 13$) and significant, because unpromoted low index planes of Pt are relatively inert toward NO dissociation (27–31) which process we propose as the key reaction-initiating step in the present case, i.e.,

$$NO_{(a)} \rightarrow N_{(a)} + O_{(a)}, \qquad [6]$$

followed by

$$CO_{(a)} + O_{(a)} \rightarrow CO_2 \qquad [7]$$

$$N_{(a)} + N_{(a)} \rightarrow N_2 \qquad [8]$$

$$N_{(a)} + NO_{(a)} \rightarrow N_2O. \qquad [5]$$

In this connection we note that low pressure kinetic studies of the CO + NO reaction over Pt by Bonzel and Pirug (6) and by Lorimer and Bell (7) support this dissociative mechanism which was previously generally accepted. However, a recent study by Klein *et al.* (9) over a wide pressure range (10^{-8}–1 Torr) led to the conclusion that the kinetic data could only be rationalized in terms of the nondissociative process $CO_{(a)} + NO_{(a)}$ as the rate determining step, although transient (low pressure) studies by Banse *et al.* (8) appear to rule out this non-dissociative mechanism. A particular difficulty with the nondissociative mechanism is that it cannot readily account for the lack of reactivity of low index planes of Pt. These disagreements regarding reaction mechanism are principally found in the high pressure regime: under low pressure conditions most available data are consistent with the dissociative mechanism. Our results strongly suggest that the dissociative mechanism holds, even in the high pressure regime. The catalyst film consists of large polycrystalline Pt particles (1) whose surfaces are dominated by (inactive) low index planes; the low rates observed in the Na-free system may be ascribed to the high index planes that are inevitably present. Na supplied to the Pt surface should strongly enhance the overall activity by inducing NO dissociation on all crystal planes. The relative effect of the Na promoter should be most pronounced on the otherwise ineffective low index planes, which of course are also the preferred adsorption sites for electropositive species. In addition to providing a rationalization for the activity data, this hypothesis is also consistent with the observed variations in selectivity. High levels of Na increase S_{N_2} because they favor reaction [6] and hence [7] and [8] as well. However, when NO dissociation proceeds to a sufficiently high degree, reaction [5] should be suppressed, as observed.

The dissociative mechanism is also firmly established by the activation energy behavior vs catalyst potential (Fig. 7b) and its one-to-one correspondence with that of the CO oxidation reaction both on the Na-promoted and on the Na-free Pt catalyst. It should be noted that, due to mass balance considerations, the sum of the rates of reactions [8] and [5], i.e., $2r_{N_2} + r_{N_2O}$, has to equal the rate of reaction [7]. Thus Fig. 7b shows conclusively that chemisorbed oxygen is an intermediate in the production of CO_2, i.e., it confirms the dissociative reaction mechanism.

Figures 5a–5c show that at intermediate values of P_{CO}, where the extent of NO dissociation is most likely to control the rate by controlling the surface O coverage, Na supply to the catalyst greatly increases the activity. At sufficiently low P_{CO} the CO + O step is limited by the restricted availability

of $CO_{(a)}$ and the EP effect should be small, as is indeed observed. At high P_{CO} the EP effect is also attenuated.

The sharp changes in activity (Fig. 6a) which occur as a function of P_{NO} at fixed potentials of −200 mV and +200 mV resemble the behavior observed for the $CO + O_2$ reaction over Pt/β'' alumina (5) and we propose an analogous explanation. At low P_{NO} the surface is dominated by islands of CO; reaction occurs only at the peripheries of these islands, resulting in a low rate. At sufficiently high P_{NO} the CO islands are disrupted by NO chemisorption, in effect a 2D phase transition, and the rate rises sharply as intermixing of the reactants occurs. This model is strongly supported by the observed effects of Na promotion. The higher the Na coverage (more negative catalyst potentials) the lower the value of P_{NO} at which the phase transition occurs, reflecting the increased strength of NO chemisorption relative to that of CO. On the electrochemically cleaned surface ($V_{WR} = +1000$ mV) the transition value of P_{NO} lies outside the experimentally accessible range. The r_{N_2} and r_{N_2O} results in Figs. 6b and 6c are similarly understandable. However, the N_2O data do exhibit an interesting difference. Although the step change in rate occur at the same values of P_{NO} for each of the products, r_{CO_2} and r_{N_2} are systematically higher as the Na coverage becomes more negative in the sequence $V_{WR} = +1000$ mV, +200 mV, −200 mV. However, the N_2O curve for $V_{WR} = -200$ mV lies in between the +1000 mV and +200 mV curves. This reflects the fact that increasing NO dissociation must always increase the rates of the O + CO and N + N reactions, whereas at a sufficiently high level of NO dissociation the N + NO rate will be retarded.

CONCLUSIONS

1. The CO + NO reaction exhibits strong electrochemical promotion under Na pumping to the catalyst when the coverages of the two reactants are comparable. In the most favorable case the rates of CO_2 and N_2 formation are enhanced over the clean surface rate by ~480% and ~1300%, respectively. This corresponds to a significant improvement in the activity of Pt toward this reaction.

2. Under all conditions, the selectivity toward N_2 formation versus N_2O production increases with decreasing catalyst potential (increasing Na coverage).

3. The above observations strongly support the view that the promoting role of Na for the CO + NO reaction is due to (a) enhanced NO vs CO chemisorption on Pt and (b) Na-induced dissociation of chemisorbed NO. The latter factor is primarily responsible for the observed very high rate enhancement ratio (ρ) and promotion index (P_{Na}) values; a corollary is that at elevated pressure the reaction proceeds by a dissociative mechanism in agreement with conclusions of UHV studies.

4. The ability of solid electrolytes, such as β-$''Al_2O_3$, to act as reversible promoter donors under the influence of the applied potential and to precisely tune the promoter coverage on catalyst surfaces allows for a systematic study of the role of promoters in heterogeneous catalysis.

ACKNOWLEDGMENTS

A.P. holds a CONICET Postdoctoral Research Fellowship. A.P. and R.M.L acknowledge support by the British Council and Fundación Antorchas. Additional support under British Council Grant ATH/882/2/FUEL and from the Hellenic Secretariat EPET-II Programme is also gratefully acknowledged.

REFERENCES

1. (a) Vayenas, C. G., Bebelis, S., Yentekakis, I. V., and Lintz, H. G., *in* "Catalysis Today," Vol. 11, No 3, p. 303. Elsevier, Amsterdam, 1992. (b) Vayenas, C. G., Jaksic, M. M., Bebelis, S., and Neophytides, S., *in* "Modern Aspects of Electrochemistry" (J. O'M. Bockris, B. E. Conway, and R. E. White, Eds.), Vol 29, p. 57. Plenum, New York, 1995.
2. Neophytides, S. G., Tsiplakides, D., Stonehart, P., Jaksic, M. M., and Vayenas, C. G., *Nature* **370**, 45 (1994).
3. Pliangos, C., Yentekakis, I. V., Verykios, X., and Vayenas, C. G., *J. Catal.* **154**, 124 (1995).
4. Matsushima, T., *J. Catal.* **55**, 337 (1978); *Surf. Sci.* **79**, 63 (1979).
5. Yentekakis, I. V., Moggridge, G. D., Vayenas, C. G., and Lambert, R. M., *J. Catal.* **146**, 292 (1994).
6. Pirug, G., and Bonzel, H. P., *J. Catal.* **50**, 64 (1977).
7. Lorimer, D'Arcy, and Bell, A. T., *J. Catal.* **59**, 223 (1979).
8. Banse, B. A., Wickham, D. T., and Koel, B. E., *J. Catal.* **119**, 238 (1989).
9. Klein, R. L., Schwartz, S., and Schimdt, L. D., *J. Phys. Chem.* **89**, 4908 (1985).
10. Rodriguez, J. A., and Goodman, D. W., *Surf. Sci. Rep.* **14**, 1 (1991).
11. Park, Y. O., Banholzer, W. F., and Masel, R. I., *Surf. Sci.* **155**, 341 (1985).
12. Banholzer, W. F., Parise, R. E., and Masel, R. I., *Surf. Sci.* **155**, 653 (1985).
13. Belton, D. N., and Scmieg, S. J., *J. Catal.* **138**, 70 (1992).
14. Belton, D. N., and Scmieg, S. J., *J. Catal.* **144**, 9 (1993).
15. Oh., S. E., Fischer, G. B., Carpenter, J. E., and Goodman, D. W., *J. Catal.* **100**, 360 (1986).
16. Obuchi, A., Ohi, A., Nakamura, M., Ogata, A., Mizuno, K., and Ohuchi, H., *Appl. Catal. B* **2**, 71 (1993).
17. Kiskinova, M. P., "Poisoning and Promotion in Catalysis based on Surface Science Concepts and Experiments," Elsevier, Amsterdam, 1992.
18. Vayenas, C. G., Bebeleis, S., Neophytides, S., and Yentekakis, I. V., *Appl. Phys.* A**49**, 95 (1989).
19. Yentekakis, I. V., Neophytides, S., and Vayenas, C. G., *J. Catal.* **111**, 152 (1988).
20. Yentekakis, I. V., and Bebelis, S., *J. Catal.* **137**, 278 (1992).
21. Harkness, I. R., Hardacre, C., Lambert, R. M., Yentekakis, I. V., and Vayenas, C. G., *J. Catal.* (1996).
22. Vayenas, C. G., Bebelis, S., and Despotopoulou, M., *J. Catal.* **128**, 415 (1991).
23. Bertolini, J. C., Delichere, P., and Massardier, J., *Surf. Sci.* **160**, 531 (1985).
24. Harkness, I. R., and Lambert, R. M., *J. Catal.* **152**, 211 (1995).
25. Harkness, I. R., and Lambert, R. M., in preparation.
26. Lang, N. D., Holloway, S., and Norskov, J. K., *Surf. Sci.* **150**, 24 (1985).
27. Gorte, R. J., Schimdt, L. D., and Gland, J. L., *Surf. Sci.* **109**, 367 (1981).
28. Lin, T. H., and Somorjai, G. A., *Surf. Sci.* **107**, 573 (1981).
29. Kiskinova, M., Pirug, G., and Bonzel, H. P., *Surf. Sci.* **136**, 285 (1984).
30. Serri, J. A., Cardillo, M. J., and Becker, G. E., *J. Chem. Phys.* **77**, 2175 (1982).
31. Campbell, C. T., Ertl, G., and Segner, J., *Surf. Sci.* **115**, 309 (1982).